The International Journal of Advanced Manufacturing Technology
https://doi.org/10.1007/s00170-018-2542-4

ORIGINAL ARTICLE

Enhancements on strength of body structure due to bake hardening effect on hot stamping steel

Marcos Roberto de Castro [1,2] · Waldemar Alfredo Monteiro [2] · Rodolfo Politano [2]

Received: 20 May 2018 / Accepted: 8 August 2018
© Springer-Verlag London Ltd., part of Springer Nature 2018

Abstract
Body structure projects are designed to develop lightweight structures, which result in low fuel consumption and emissions for internal combustion engines and longer battery life in the case of electric vehicles. The structures need to be lightweight but also strong in order to provide maximum safety to the occupants. These premises have led to the development of special materials such as the hot stamping steels. The most used steel in this process, quenched 22MnB5, also exhibits the bake hardening effect: its yield stress increases after being exposed at temperatures close to 200 °C (typical heat treatment of paint lines in the automotive industry). The aim of this study was to verify the improvement in the mechanical strength of a body structure due to the bake hardening effect to which the hot-stamped steel components were submitted. Samples of annealed 22MnB5 steel were submitted to tensile and chemical analysis. A second group of the same steel was subjected to an additional heat treatment in a laboratory furnace simulating the heating that occurs in the body paint line. Subsequently, the same tests were performed with the samples from the first group. Tensile tests evidenced the increase of 6.5% in the yield stress of the samples that suffered the bake hardening effect. The stress-strain diagram curves were used as the input to the side crash simulation program. The simulations demonstrated that the body structure whose hot-stamped parts were subjected the bake hardening effect had a 2% reduction in side crash intrusion compared to body structure where the parts did not suffer this effect. In the case of the lateral protection bar test, the bake hardening effect provided a 5% increase in the maximum bending load.

Keywords Hot stamping · Bake hardening · High-strength steels · Press hardening steel

1 Introduction

Oil crises in the 1970s drove the automotive industry's to reduce dependence on fossil fuels: improving the energy efficiency of the powertrain, reducing aerodynamic drag of bodies, and reducing vehicle mass. At the same time, studies were developed on the vulnerability of vehicle occupants in case of impact and on design concepts to minimize damages [5]. By imposing legislation, engines cannot exceed emission levels of increasingly restrictive emissions and vehicles must provide safety to occupants in the event of a collision. This protection can be achieved, inter alia, by means of crash tests. Traffic accidents are responsible for thousands of victims, and those caused by side crashes account for about crash are 30% of them [13].

The use of special materials is one of the ways of combining mass reduction with the increase in structural stiffness and strength against crashes on vehicle. Among the high-strength steels, steels of two or more phases and hot-stamped steels are inserted.

This work aims to study the bake hardening effect on the 22MnB5 steel used in the hot stamping process. This effect is well known in this grade of steels, but here, the improvement in mechanical strength that it measured by means of side crash simulations and the impact bar test will be quantified. This evaluation will be made comparing the results between two identical bodies with

✉ Marcos Roberto de Castro
Marcos.castro@volkswagen.com.br

Waldemar Alfredo Monteiro
wamontei@ipen.br

Rodolfo Politano
Politano@ipen.br

[1] Volkswagen do Brasil, São Paulo, Brazil

[2] Nuclear and Energetic Researches Institute, University of São Paulo, São Paulo, Brazil

Published online: 28 September 2018

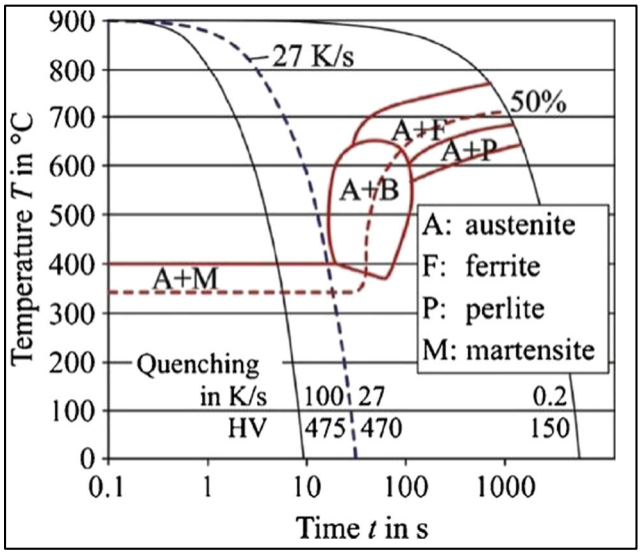

Fig. 1 Continuous cooling diagram of 22MnB5 [9]

quenched 22MnB5 steel parts, in which one of these components will be subjected the bake hardening effect.

1.1 Hot stamping

Hot stamping allows complex geometries to be obtained using considerably lower press loads than in cold forming [6]. At the end of the process, the steel used undergoes transformation in the microstructure and its strength is greatly increased: yield stresses above 1100 MPa. Such strength allows the use of thinner sheets (compared to cold-formed parts). Among the steels for hot stamping, 22MnB5 is the most commonly used [9]. This material is supplied with perlite microstructure with ultimate tensile strength up to 600 MPa. After completion of the hot stamping process, the ultimate tensile strength can reach 1500 MPa. After being austenitized, the blank is formed and cooled simultaneously. The cooling is done by a system (in the drawing tool) that uses cold water and lasts for 5 to 10 s [10]. The cooling rate must be at least 27 K/s until the temperature drops to 400 °C, so that a non-diffusion transformation is induced, resulting in the high mechanical strength of the product (Fig. 1).

The mechanical properties of the steel after quenching depend on the proportion of carbon in the alloy. Elements such as Mn and Cr improve the mechanical strength after quenching, but boron is the chemical element that most influences the hardenability, when it is fixed in the contour of the austenitic grains. Boron delays the transformation of austenite to more ductile structures, which favors martensitic transformation [9]. Some automotive applications of hot stamping are A-pillar, B-pillar, side impact bar, sill, frame components, bumper elements, door reinforcing bars, roof frame, tunnels, front and rear frames, and crossbars (Fig. 2). The thicknesses of these sheets vary from 1 to 2.5 mm.

1.2 Bake hardening effect

Bake hardening steels are those which acquire an increase in yield stress when exposed to temperatures of about 170 °C for 15 or 20 min. This heat treatment coincides with what happens in most of the driers of automotive paint lines [6]. There is considerable amount of soluble carbon available in continuous annealing lines. During the heat treatment, they migrate to the dislocations by fixing them: they are the so-called Cottrell atmospheres [5]. This influence the movement of dislocations, which requires more effort to cause deformation (Fig. 3).

The interaction of solute atoms with dislocations can be verified by means of the internal friction technique [3]. Internal friction can be defined as the ability of a material to dampen mechanical vibrations [14]. In this technique, sample heating provides the necessary energy for the diffusion of the interstitials at the same time that stress is cyclically applied. With the anchoring of the dislocations, the deformation recovery time changes after the stress is removed [2].

An ideal material, free from defects in the microstructure, exhibits elastic behavior property: when a stress is applied (be it tensile, compression, twist, or bending) within the elastic field, a corresponding deformation arises. If the stress is no longer applied, the recovery of the deformation is complete

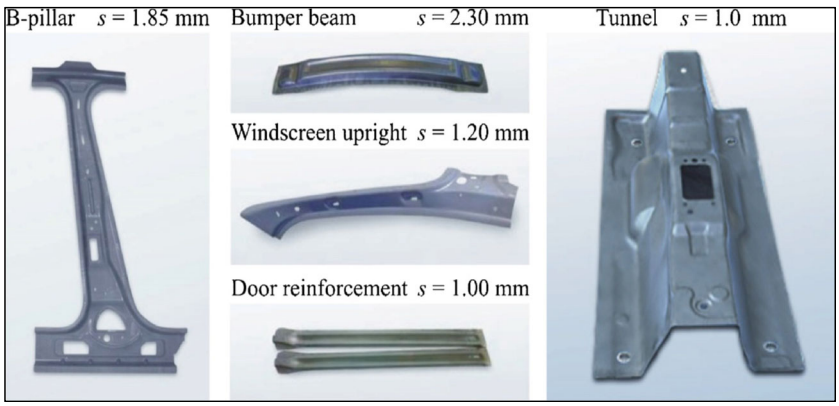

Fig. 2 Hot-stamped parts [9]

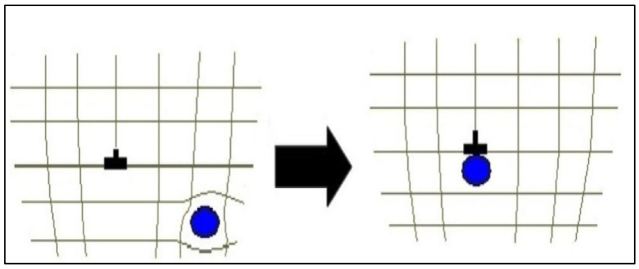

Fig. 3 Representation of the formation of the Cottrell atmospheres [15]

and instantaneous. With the presence of discordances, interstitial atoms, substitutional atoms, and other defects, recovery is complete, but not instantaneous [12]. In the case of cyclic stresses, the internal friction [Q^{-1}] is given by the formula:

$$Q^{-1} \times \pi = \delta = \ln \frac{A_n}{A_{n+1}}$$

A_n amplitude of cycle vibration
A_{n+1} amplitude of the vibration of the next cycle

1.3 Body structure

The body structure is composed by the luggage compartment, the protection to the occupants, and the integration of several systems. The concept of integrated structure was born with the idea of sharing the vehicle body into three distinct zones: frontal deformation zone, rear deformation zone, and survival cell (Fig. 4).

According to Malen [11], the structural requirements of the bodies are as follows:

- Stiffness: describes controlled deformation under normal repeated loading;
- Resistance: describes the maximum load in extreme applications where some permanent deformations are expected;
- Energy absorbed by the structure: it deals with loading and the evolution of the deformation in case of severe impacts.

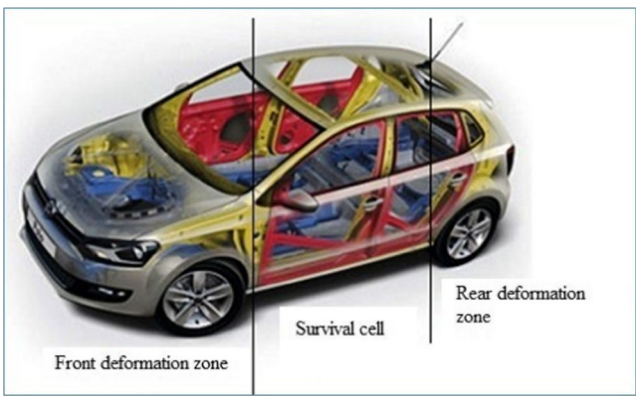

Fig. 4 Deformation zones

Crash tests are performed to ensure the integrity of the vehicle and primarily of the occupants in the event of a collision [13]. Side impact tests may be of the vehicle colliding against barriers (deformable or not) and against a pole. One of the tests involves a collision between and a vehicle and a barrier at a speed of 50 km/h (Fig. 5).

2 Materials and methods

2.1 Mechanical properties

The main parameters of the stamping sheets are obtained through the tensile test [8]. Some of the samples were heated and then air-cooled prior to the test, simulating the passage of the components in the paint driers. The tensile tests provide stress-strain curves. The stress in this case is the so-called engineering stress. For its use in finite element software, such as structural analysis, it was necessary to calculate the true stress (σ_v) obtained by Holloman's law:

$$\sigma_v = K\,\varepsilon_v{}^n$$

where

K (plasticity constant) and n (work hardening coefficient) material constants
ε_v true strain

The quenched samples were supplied by the Brazilian steel company Usiminas, (laser-cut) as specimens with a thickness of 1 mm (Fig. 6).

For each group of five samples, the thermal treatments used were as follows:

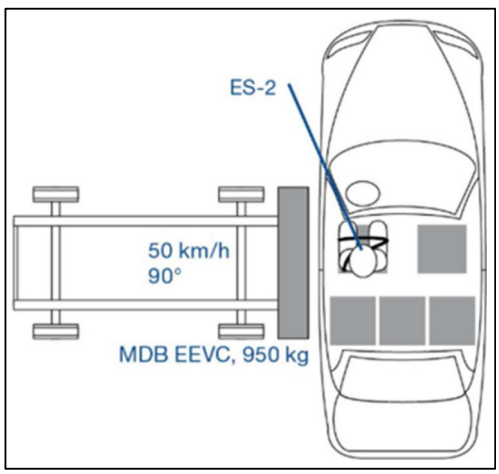

Fig. 5 Side crash tests according to ECE-R95 [13]

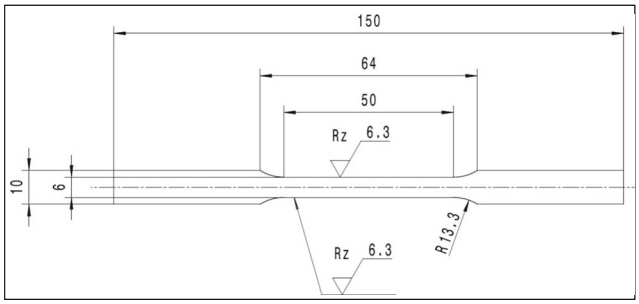

Fig. 6 Sample for tensile test

(i) heating to 170 °C. Maintained at this temperature for 20 min. Air cooling followed. This treatment is close to the standards used in automobile dryers.
(ii) heating to 170 °C. Maintained at this temperature for 30 min. Air cooling followed.
(iii) heating to 170 °C. Maintained at this temperature for 40 min. Air cooling followed.
(iv) heating to 190 °C. Maintained at this temperature for 20 min with subsequent cooling to air.

Optical microscopy of the material was performed using light field techniques. The preparation was done with sanding, polishing, and etching with 10% nital. After the rupture of the specimens in the tensile tests, fractographic studies were carried out by means of scanning electron microscopy.

2.2 Side crash test simulation

The ESI: Pam-Crash 2014.05 side crash simulation software was used. The simulation mesh used 2D elements of the shell type (four nodes) and 3D elements (eight hexagonal nodes). The time-step was 0.5 microseconds. The properties of the analysis are deformable materials and strain rate considered.

In the mathematical model, the parts using this material were reinforcement B-Pillar, side impact bar, threshold, and longitudinal reinforcement between the roof and the side (Fig. 7). With the results of the simulation, the effect of the heat treatment on the body of a virtual vehicle based on a compact model was verified.

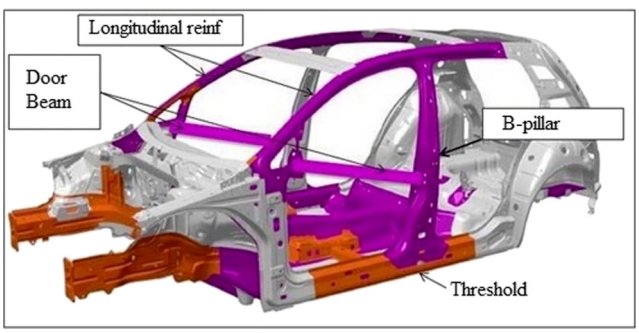

Fig. 7 Body structure [1]

This comparison was made by measuring the intrusions at six points: three in the region of B-Pillar and three in the region of the inner panel of the door. The inner panel of the door is not made of 22MnB5 steel, but is deformed in case of side crash. Among these components, the most requested in case of lateral impact is the B-Pillar, integrated into the body by means of spot welding in the stage of the known manufacturing process by frame. After the frame, the body goes to painting line.

2.3 Chemical analysis

The chemical characterization of the material was done by optical emission equipment. Atoms excited by an external source of energy, in this case, a source of monochromatic light, have the orbits of their electrons shifted, with changes in their state of energy. For each chemical element, there are special spectral ray characteristics [7].

2.4 Internal friction test

Still in the part of physical metallurgy, internal friction analysis was done in the equipment known as dynamic mechanical analyzer (DMA) to verify the interaction of alloying element (carbon) with the dislocations. Rectangular samples measuring 4 × 55 mm were supported on two points and subjected to cyclic stresses by stamp acting at the midpoint, which characterizes bending.

The equipment of the brand Netzsch (Fig. 8) applies cyclic stresses at frequencies of 0.5, 1, 2, and 5 Hz.

Fig. 8 Equipment for internal friction test

Fig. 9 Side crash bar in 22MnB5 quenched steel

The presence of surface coating may affect the result of the internal friction analysis. Therefore, the samples were sanded in order to remove the scuff and the surface coating. During the test, the samples were heated at a rate of 1 °C min^{-1} from room temperature to 180 °C. This temperature was maintained for 20 min. Cooling was then continued in air to room temperature. The DMA equipment displays a Cartesian graph with temperature in the abscissa axis and the quantity tan δ on the ordinate axis. As mentioned earlier in this chapter, internal friction indicates the ability of the material to dampen mechanical vibrations or energy dissipated under stress. If the stresses are cyclic, the time lag in the recovery of the deformation is given by the angle δ which is equal to the natural logarithm of the quotient of the amplitude of the vibration of one cycle by the deformation of the vibration of the next cycle. Simultaneously, this equipment registers the value of modulus of elasticity that tends to suffer small reduction in this temperature range due mainly to the relief of stresses. In this work, the temperature reached was 180 °C. Samples were maintained at this temperature for 20 min.

2.5 Side crash bar bending test

One of the tests to evaluate the mechanical strength of the body is the side crash bar bending test, which is inside the driver's door (Fig. 9).

This test is based on the FMVSS 214 standard. In this evaluation, four quenched 22MnB5 steel bars were supported in equipment of the brand Instron (maximum load 100 kN). The supports were spaced 720 mm apart. At the midpoint between the supports, a punch with a circular section (radius of 127.5 mm) acts perpendicularly against the bar with a speed of 4 mm/s (Fig. 10).

The machine generates a graph which registers the load to bend the bar as a function of the displacement caused by the punch. Before the bending tests, two of the bars were exposed in an oven at 190 °C for 20 min and then cooled to air.

3 Results and discussion

3.1 Optical microscopy

The microstructure was the typical martensitic morphology. The martensite, a product of hot stamping, has low angle between laths and high angle between packets [4]. There were no changes in the microstructure in the comparison of the only quenched material (Fig. 11a) with the quenched material that suffered the bake hardening effect (Fig. 11b).

3.2 Chemical analysis

The chemical analysis of quenched 22MnB5 steel (five points of analysis) by means of the optical emission equipment had the following results (Table 1):

The elements that compose the binary alloy of basic steel are iron and carbon, the latter traditionally hardener of the alloy. Other important elements found were as follows: manganese, responsible for improving the hardenability; the niobium, considered an element that contributes to avoid the embrittlement by hydrogen; and the titanium to which the purpose is, among others, to combine with the nitrogen so that it does not combine before with boron. It should be noted that boron is the alloying element that gives name to the class of steels for hot stamping, due to its characteristic of being fixed

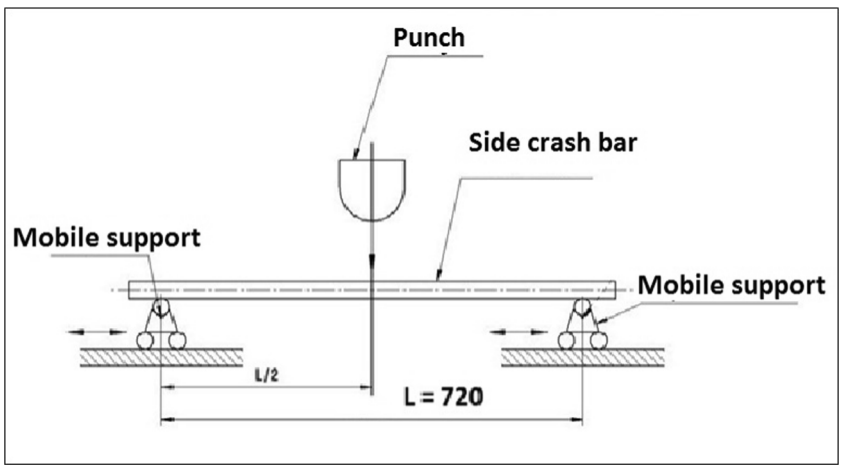

Fig. 10 Side crash bending test according to FMVSS 214 [16]

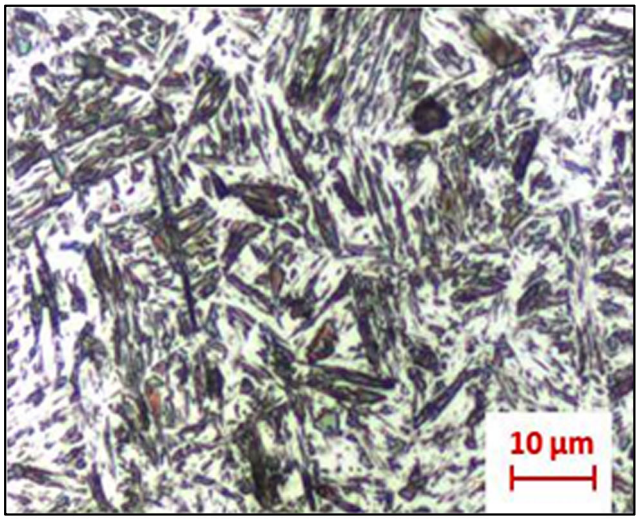

(a)

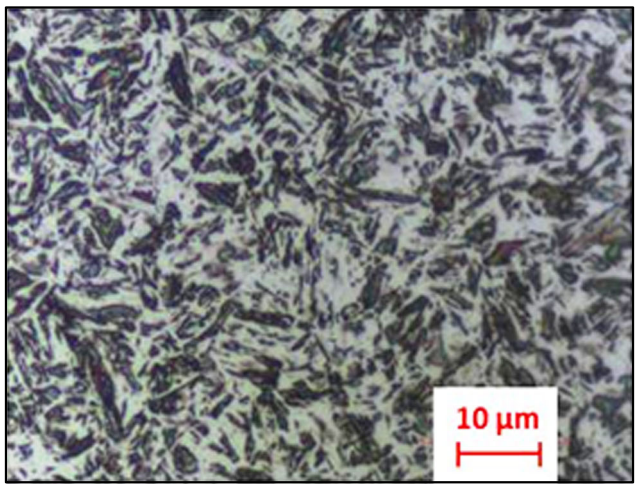

(b)

Fig. 11 Optical microscopy of quenched 22MnB5 steel (**a**) and the material with post bake hardening (**b**): nital 10%

in grain contours stabilizing austenite: martensitic transformation occurs at lower cooling rates compared to steels without alloying elements.

3.3 Tensile tests

The specimens were submitted to the uniaxial tensile test with deformation rate of 36 min^{-1}. This rate is in accordance with the ISO 6892-1 standard.

Figure 12 shows the results of the ultimate stress and yield stresses obtained. The tensile test for the first group of samples was done without further heat treatment. In the following condition, the samples underwent a heat treatment similar to that in the paint dryer (the temperature of 170 °C was maintained for 20 min): unlike the steels classified as bake hardening (BH), there was no gain in mechanical strength. Maintaining the temperature of 170 °C and increasing the time to 30 min,

Table 1 Chemical composition of quenched 22MnB5 steel

Element	% (weight)
C	0.249
Si	0.235
Mn	1.20
P	0.02
S	0.0021
Cr	0.237
Ni	0.0095
Mo	0.002
Al	0.050
Co	0.0015
Ti	0.051
Nb	0.0031
V	0.006
W	0.010
B	0.0043
Mg	0.001
Pb	0.003
Sn	0.0019
Zn	0.008
Bi	0.0027
Zr	0.004
Cu	0.010
Fe	97.9

there was a slightly more representative gain in the yield strength. At 40 min, the gain was 93 MPa. Turning the duration to the time condition of the first heat treatment (20 min), but increasing the exposure temperature (190 °C), the gain was equally significant: 86 MPa.

The increase in yield stress by bake hardening is accompanied by a small reduction in the ultimate stress. If on the one hand the mechanical resistance is increased by the anchoring of dislocations by the carbon atoms, on the other hand, there is the relief of stresses, induced by the increase in the temperature of the material.

Changing the time-temperature pairs, by bake hardening effect, the tensile tests revealed a gain close to 100 MPa in the yield stress, accompanied by a small loss in the ultimate stress. The yield stress in the present study is more important than that of resistance, because the higher its value, the more stiff the structure is. The ultimate stress, when exceeded, indicates the total collapse and in this case had a small decrease. The elongation did not change significantly (Fig. 13).

Therefore, considering the time-temperature pair 170 °C for 20 min (common in the driers of the paint line), the improvement in mechanical property was not significant. Maintaining this temperature for longer, or maintaining the time with higher temperature, the gain was expressive in absolute values. In percentage terms, however, the improvement

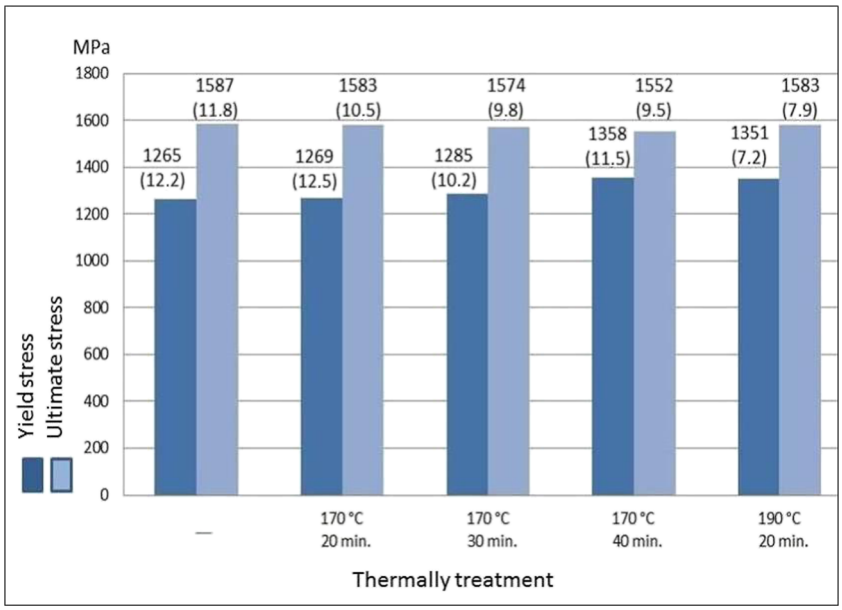

Fig. 12 Mean values of yield stresses and ultimate stresses obtained in the tensile tests (values in parentheses refer to standard deviations)

was slightly above 6% in the yield stress. With the data obtained in the tensile test, the time-temperature pair chosen for the later stages of this study was as follows: heating at 190 °C for 20 min, followed by air cooling.

3.4 Fractography analysis

After the tensile tests, a study was made by electronic fracture (scanning electron microscopy). The test specimens had a small stent before the fracture (Fig. 14).

In the microstructural aspect, the fracture region exhibited irregular shapes, with some alveolar portions. This, although the elongation of the material is only 6% and is thus slightly above the elongation, corresponds to the yield stress (2%). High-strength steels and low elongation tend to have fragile fracture characteristics, where the fracture is of the transgranular type (cleavage), since fracture cracks pass through the grains.

The analyzed samples showed a fragile fracture, but with a ductile fracture mechanism. In the specimens analyzed, the numerous spherical microcavities are characteristics of uniaxial traction failure, which is the case of the traction test. In Fig. 15, the images generated by the scanning electron microscopy show, in addition to the dimples, some voids formed by the coarsening of the wells that can indicate the beginning of the material failure at the moment the maximum tensile strength was reached. It was observed, as occurred in optical microscopy, that there were no significant changes between the sample of tempered material and the sample of tempered material with subsequent bake hardening.

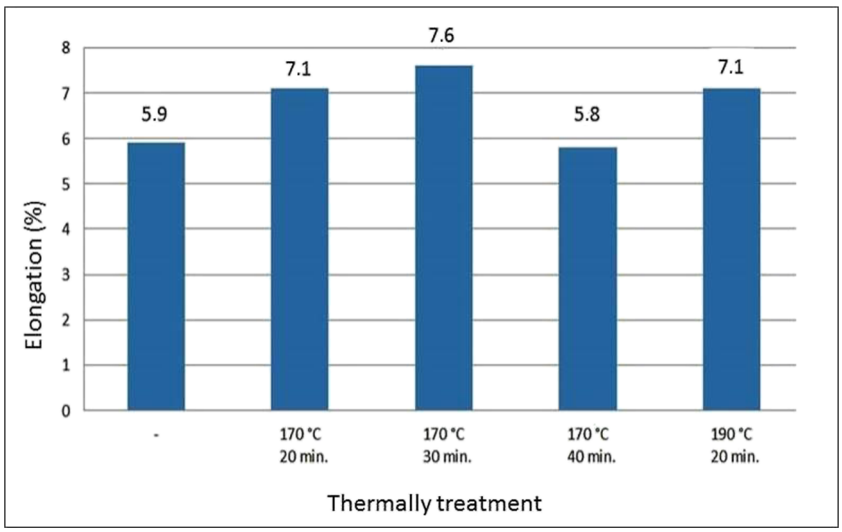

Fig. 13 Mean values of the elongation corresponding to the applied thermal treatments

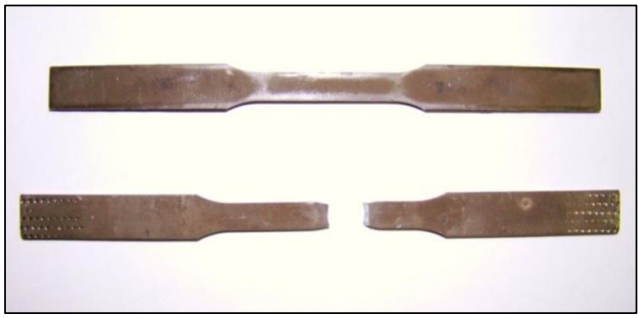

Fig. 14 Test specimens (before and after tensile test) in quenched 22MnB5 steel

3.5 Internal friction analysis

By means of Fig. 16, it is possible to verify a clear increase in tangent delta (tan δ) as the temperature approaches the temperatures where the bake hardening occurs. This increase occurs in the four frequency bands. The technique used shows the movement of the carbon in the temperature range studied: from the room temperature up to about 140 °C the internal friction undergoes little variation and then increases according to the elevation of temperature. Above this temperature, the energy is sufficient to activate the movement of the interstitials. The temperature range used in this experiment is well below the phase change temperature of the material, so the decrease in modulus of elasticity due to heating is small.

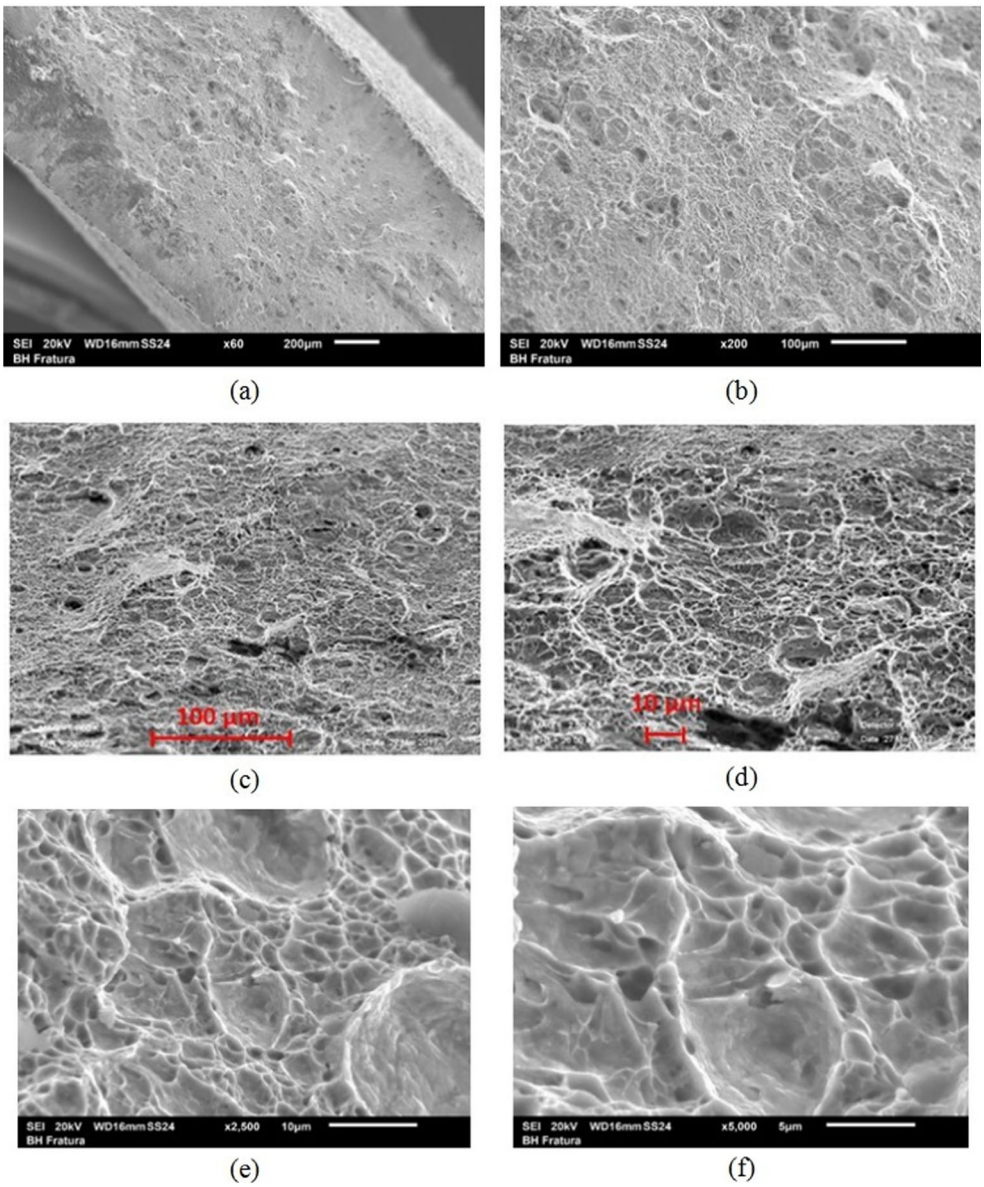

Fig. 15 Scanning electron micrographs of fracture regions of tempered 22MnB5 steel and subsequent bake hardening (nital 10%). Presence of precipitates inside dimples

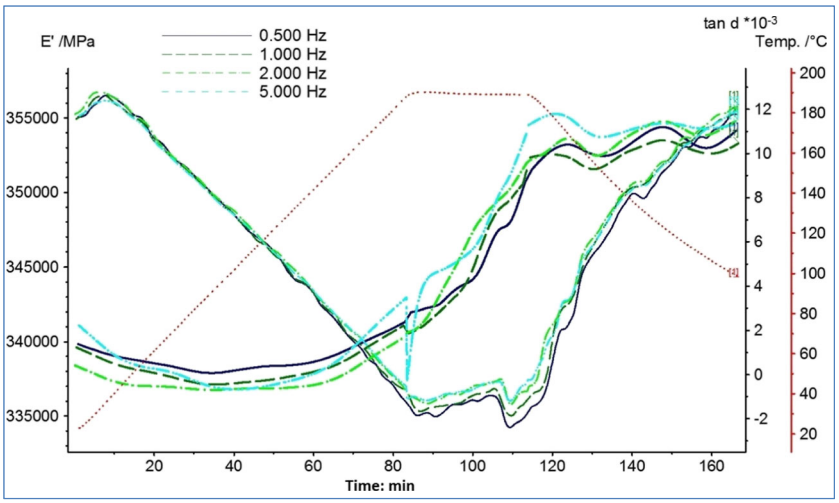

Fig. 16 Graph generated by the internal friction analysis equipment. The dotted curve describes the temperature variation. In the axis of the abscissa, the time scale and in the ordinate, on the left, the modulus of elasticity and on the right at tan δ, magnitude related to the internal friction

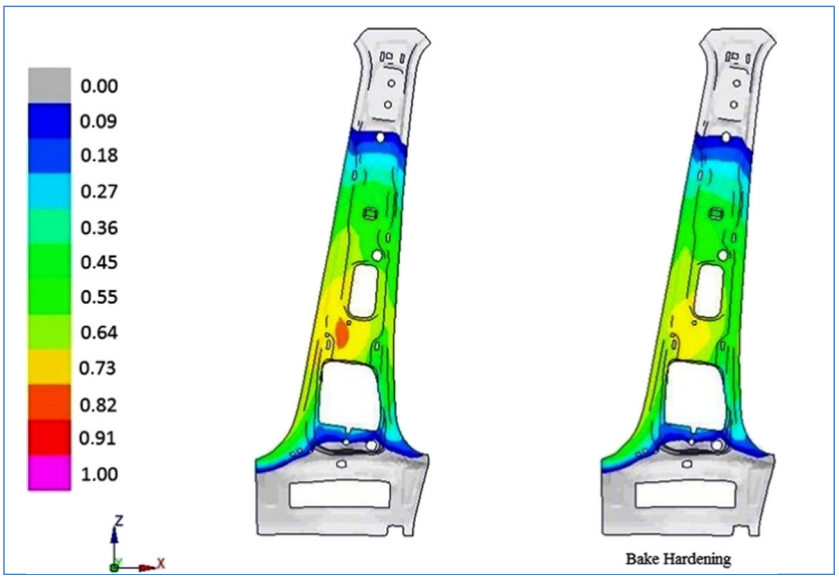

Fig. 17 Simulation of side impact: intrusions in B-Pillar

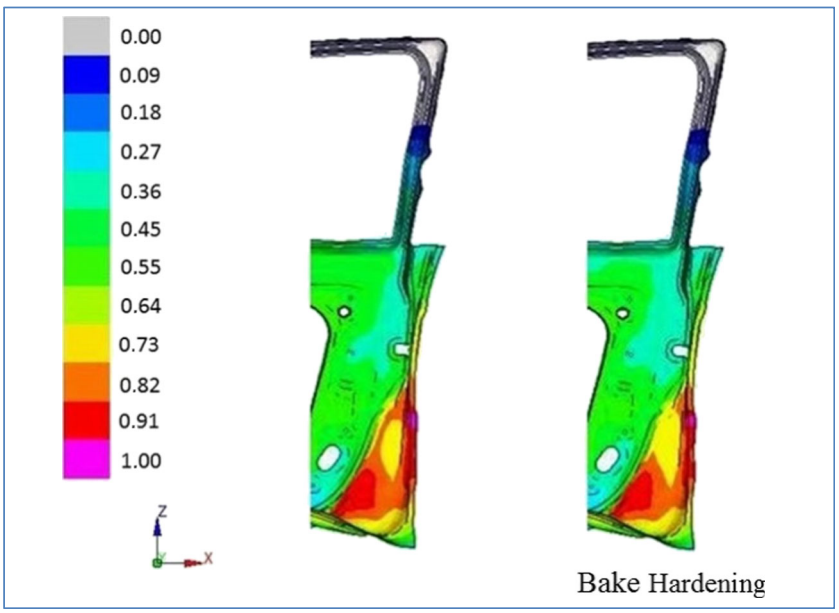

Fig. 18 Side impact simulation: intrusion on the inner door panel

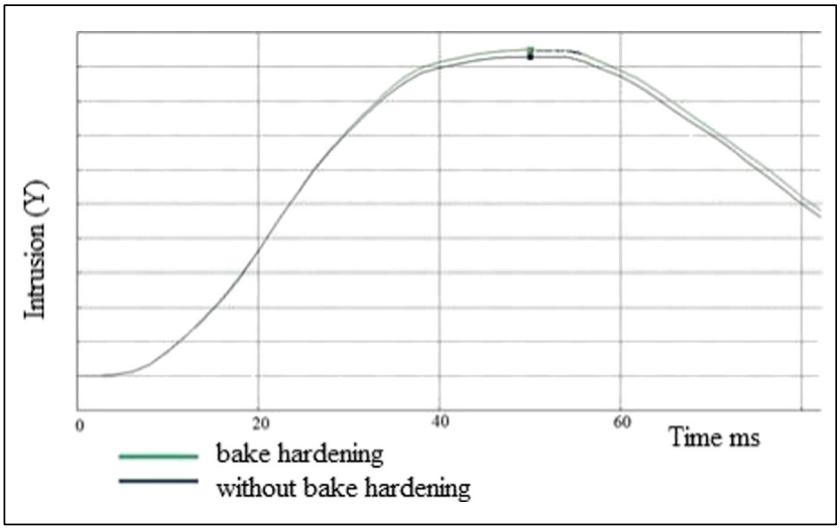

Fig. 19 Intrusion plot vs. time after impact

With cooling, the modulus of elasticity rises to near its value before the experiment while the internal friction does not return to its initial value. This can be explained by a rearrangement of the crystalline structure: the carbon atoms migrated to the dislocations. Compared to the initial condition of the experiment, the material responds differently to the application of stress. The lag between tension and deformation increases.

3.6 Side crash simulation

The stress-strain curves obtained in the tensile tests were used as input data for the Pam-Crash software for side crash simulations against barriers. The two conditions chosen for comparison were room temperature and heat treatment at 190 °C for 20 min. To study the regions that suffered intrusion, the reinforcement that is welded under the B-Pillar was taken, because among the components of the fixed part of the body, this is the metal part closest to the occupants. Here are the comparative results:

Graphically (Fig. 17), it is possible to identify a region of greater intrusion (orange color) of the piece to the left, which did not suffer bake hardening compared to the treated part. The maximum intrusion was 2% lower in the part that suffered the bake hardening effect. This intrusion amounts to about 4 mm in absolute terms. In addition to the maximum intrusion, comparatives were collected in the intrusions in three more points:

(i) Region close to the head: reduction in intrusion of 2.1%;
(ii) Region close to the shoulders: also showed a reduction in intrusion of 2.1%;
(iii) Region near the threshold: there was no reduction in intrusion.

Fig. 20 Side crash bar after bending

The internal panel of the door was then analyzed, next to B-Pillar. Intrusions were collected in three points: shoulder region, near the threshold, and in the intermediate region between the first two. The inner door panel is not made from quenched 22MnB5 steel, but is intruded on side impact.

In Fig. 18, it is possible to identify that the intrusions were greater in the part that did not suffer bake hardening: the area in the orange color covers a portion that does not appear in the piece to the right of the image. The reduction in intrusion was also around 2%. In the three points collected for comparison, the following were obtained:

(i) Region close to the shoulder: reduction in intrusion by 1.8%;
(ii) Region near the threshold: reduction in intrusion by 1.1%;
(iii) Reduction in the midpoint between the two regions described above: reduction in intrusion by 1.5%.

The side crash simulations revealed maximum intrusions in the time of 50 m/s after the collision, as shown in the graph of Fig. 19.

Table 2 Loads and maximal displacements obtained in bending tests

Samples	Max. load [N]	Displacement [mm]
1	11,679.4	23.8
2	11,685.2	22.9
3	12,302.6	22.3
4	12,309.4	21.8

Bars 1 and 2: without bake hardening

Bars 3 and 4: with bake hardening

3.7 Side crash bar bending test

The test caused plastic deformation localized mostly at the midpoint of the workpiece (Fig. 20).

The results obtained in this test are in Table 2.

The results showed an increase of about 600 N in the maximum loading of the parts that suffered the bake hardening effect (3 and 4) compared to those that were not subjected to this effect (1 and 2), which represents an improvement of 5%: almost the increase observed in the tensile tests (6.5%). The extent of displacement, which can be translated by intrusion, had small decreases.

Analyzing the graph generated by the side crash bar bending test (Fig. 21), in addition to the pure values of the loads and the maximum extent of compression, it is noted that the four bars follow the same deformation line up to just over 20 mm. In the two bars that underwent the additional heat treatment, the extension of the deformation is characterized by an extension of this line, which is equivalent to about 600 N.

In the graph, it was also possible to verify the presence of a loading plateau in the four bars: the maximum loading remained constant while the intrusion of the punch in the part was observed from 20 to 40 mm.

In the two thermally treated parts, there was an increase in the energy of absorption of impact at the end of the ascending part of the curve represented by a peak. After overcoming the additional resistance, the value of the bending load resembled that of the parts without bake hardening.

After the loading step obtained in the four-bar test, the extent of compression increases even at lower loading: the plastic deformation increases in such a way that the structural collapse of the part occurs.

4 Conclusions

(1) Quenched 22MnB5 steel samples exhibited the bake hardening effect after heat treatment like that in automotive paint lines.

(2) Structural maintenance between the parts with and without additional heat treatment in 22MnB5 steel samples.

(3) Considering the usual time-temperature pair of the paint lines (170 °C for 20 min), the bake hardening effect was more significant by increasing the time (170 °C for 40 min) or the exposure temperature of the samples to the heat treatment (190 °C for 20 min). In both situations, the yield strength increased by 6.5%. Further studies can analyze the phenomena on other hot-stamped steel grades subjected to other time-temperature pairs, with special attention in industrial applications, whereas body structures has structural adhesives and their functional maximum temperature normally not exceed 200 °C.

(4) Comparing the side crash simulations between two bodies with 22MnB5 hot-stamped steel parts, the body whose parts suffered the bake hardening effect had a 2% lower lateral intrusion.

(5) The side crash bar bending test revealed that the part whose material had the bake hardening effect required

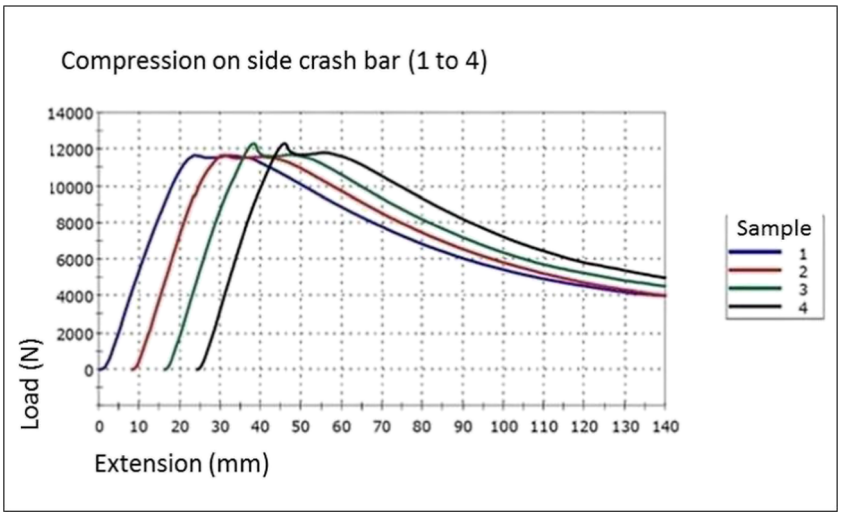

Fig. 21 Diagram generated by side crash bar bending test

600 N more than its corresponding bars without the additional heat treatment to reach its maximum displacement: an increase of 4%.

(6) With the applied internal friction test, it is possible to verify (identify) the mechanism of the interstitial atoms diffusion interacting with the dislocations in the temperature ranges of the automobile paint driers (bake hardening process).

Acknowledgements The authors would like to thank Energetic and Nuclear Researches Institute—IPEN, Volkswagen do Brasil, Volkswagen Kassel (Germany), Schuler Presses, Usiminas, Gestamp, and Benteler.

Publisher's Note Springer Nature remains neutral with regard to jurisdictional claims in published maps and institutional affiliations.

References

1. Alsmann M (2013) Warmumformung – Herstellung höchfestersicherheits-relevanter Strukturbauteile. Seminary Volkswagen A.G, Merseburg (Germany)
2. Blanter, M.; Neuhäuser, H.; Golovin, I.; Sinning, H.; *Internal friction in metallic materials*. Springer, Berlim – Heidelberg (Germany), 2007
3. Cooman B, Fan D (2011) State-of-the-knowledge on coating systems for hot stamped parts. Steel research international, Weinheim (Germany)
4. Cooman, B.; Kwon, H.; Choi, W.; Lee, J.; Bake hardening analysis of 22MnB5 PHS by the impulse internal-friction. Hot sheet metal forming of high-performance steel congress. Toronto (Canada), 2015
5. Davies G (2012) Materials for automobile bodies, 2nd. edn. Elsevier, Waltham (United Kingdom)
6. Gorni, A. Novos aços ferríticos garantem alta resistência e conformabilidade a chapas finas laminadas a frio. Corte e Conformação Magazine, Aranda, São Paulo (Brazil), 2010 **(in Portuguese)**
7. Hayakawa, M.; Kajita, T; Jeszensky, G. *Análise química de aços por espectrometria de emissão ótica*. Sorocaba (Brazil), 1980 **(in Portuguese)**
8. Hosford WF, Caddell RM (2011) Metal forming mechanics and metallurgy. New York (USA), Cambridge
9. Karbasian H, Tekkaya AE (2010) A review on hot stamping. Journal of Materials Technology, Elsevier, Dortmund (Germany)
10. Lundström E (2013) 30-year experience in press hardening. Seminary Schuler Press, São Paulo (Brazil)
11. Malen DE (2011) Fundamentals of automobile body structure design. SAE International, Warrendale (USA)
12. Meyers M, Chawla K (2010) Mechanical behavior of materials, 10ª. edn. New York (USA), Cambridge
13. Prado GI, Pereira EA, Lacerda RM (2013) Comparative analysis of side impact tests, tendencies and challenges for Brazilian market. Congress SAE, São Paulo (Brazil)
14. Ritchie, I. G., Mathew, P. M., Pan, Z. I. Osborne, C. and Prikryl, J. K., Mechanical relaxation spectroscopy in steel wire research**.** Wire Journal International p 201–218, 1989
15. Rodrigues Jr J., Influência das temperaturas de encharque e superenvelhecimento nas propriedades mecânicas de um aço ultra baixo carbono com características BH processado via recozimento contínuo. Master of Science paper. Federal University of Minas Gerais, Belo Horizonte (Brazil), 2010 **(in Portuguese)**
16. U.S. Department of Transportation. *Federal motor vehicle safety standards – evaluation,* Virginia: National Technical Information Service, 1999 (FMVSS 214)